Syncytin-A knockout mice demonstrate the critical role in placentation of a fusogenic, endogenous retrovirus-derived, envelope gene

Anne Dupressoir[a,1], Cécile Vernochet[a,1], Olivia Bawa[b], Francis Harper[c], Gérard Pierron[c], Paule Opolon[b], and Thierry Heidmann[a,2]

[a]Unité des Rétrovirus Endogènes et Eléments Rétroïdes des Eucaryotes Supérieurs, Unité Mixte de Recherche 8122, Centre National de la Recherche Scientifique, Institut Gustave Roussy, 94805 Villejuif, and Université Paris-Sud, 91405 Orsay, France; [b]Vectorologie et Transfert de Gènes, Unité Mixte de Recherche 8121, Institut Gustave Roussy, 94805 Villejuif, and Université Paris-Sud, 91405 Orsay, France; and [c]Laboratoire de Réplication de l'ADN et Ultrastructure du Noyau, Formation de Recherche en Evolution 2937, Institut André Lwoff, 94801 Villejuif, France

Edited by John M. Coffin, Tufts University School of Medicine, Boston, MA, and approved May 21, 2009 (received for review March 17, 2009)

In most mammalian species, a key process of placenta development is the fusion of trophoblast cells into a highly specialized, multinucleated syncytiotrophoblast layer, through which most of the maternofetal exchanges take place. Little is known about this process, despite the recent identification of 2 pairs of envelope genes of retroviral origin, independently acquired by the human (*syncytin-1* and *syncytin-2*) and mouse (*syncytin-A* and *syncytin-B*) genomes, specifically expressed in the placenta, and with in vitro cell–cell fusion activity. By generating knockout mice, we show here that homozygous *syncytin-A* null mouse embryos die in utero between 11.5 and 13.5 days of gestation. Refined cellular and subcellular analyses of the *syncytin-A*-deficient placentae disclose specific disruption of the architecture of the syncytiotrophoblast-containing labyrinth, with the trophoblast cells failing to fuse into an interhemal syncytial layer. Lack of *syncytin-A*-mediated trophoblast cell fusion is associated with cell overexpansion at the expense of fetal blood vessel spaces and with apoptosis, adding to the observed maternofetal interface structural defects to provoke decreased vascularization, inhibition of placental transport, and fetal growth retardation, ultimately resulting in death of the embryo. These results demonstrate that *syncytin-A* is essential for trophoblast cell differentiation and syncytiotrophoblast morphogenesis during placenta development, and they provide evidence that genes captured from ancestral retroviruses have been pivotal in the acquisition of new, important functions in mammalian evolution.

cell–cell fusion | placenta | syncytiotrophoblast | embryonic lethality | mammalian evolution

The placenta is an autonomous and transient organ of embryonic origin (same genotype as the embryo), essentially intended for feeding and oxygenating the fetus during intrauterine life. In several mammalian species with a hemochorial placenta, including the human and mouse, the fusion of trophoblast cells into a multinucleated layer called the syncytiotrophoblast constitutes a key process of placental morphogenesis (1–4). The syncytiotrophoblast is the main fetomaternal barrier in direct contact with the maternal blood, mediating the essential trophic exchange functions between the mother and the fetus, along with hormone production and protection of the fetus against the mother's immune system. Remarkably, syncytiotrophoblasts are found in the placenta of diverse species belonging to all 4 eutherian superorders, consistent with a convergent evolution process and the presence of strong selective pressures that favor this structure (5, 6). Yet, the molecular mechanisms underlying the convergent emergence of the syncytiotrophoblast remain speculative. Vertebrate genomes harbor thousands of endogenous retrovirus (ERV) elements that display a structure close to that of the integrated proviral form of exogenous retroviruses (*gag*-, *pol*-, and *env*-related regions flanked by 2 LTRs) and that most probably are the remnants of past infections of the germ line by ancestral retroviruses (7, 8). Although the majority of these elements are defective, a few of them still contain intact ORFs, notably in *env* genes. A systematic search through the human genome has identified *syncytin-1* and *syncytin-2*, 2 *env* genes that entered the primate lineage 25 million to 40 million years (Myr) ago, are specifically expressed in the placenta, and show in vitro cell–cell fusogenic activity involving a mechanism related to *env*-mediated viral cell entry (9–11). Subsequently, the existence of 2 murine endogenous retroviral *env* genes, *syncytin-A* and *syncytin-B*, homologous but not orthologous to the human syncytin genes, was reported (12). These genes entered the rodent lineage 20 Myr ago and exhibit properties similar to those of the human syncytin genes: they are specifically expressed in the placenta, at the level of the syncytiotrophoblast-containing labyrinthine zona where the feto-maternal exchanges take place, and they induce cell–cell fusion in transfected cell cultures, probably through interaction with distinct receptors (12). Discovery of syncytin genes in the mouse now allows a definite assessment of the role of these genes in mammalian physiology via knockout mouse mutants. Here, we generated a first series of knockout mice for one of the syncytin genes, *syncytin-A*. We found that homozygous null embryos die in utero between embryonic days 11.5 and 13.5, providing evidence that *syncytin-A* is essential for mouse embryonic development. Living null embryos disclose fetal growth retardation, a decrease in vascularization, and a reduction in placental transport function, leading to miscarriage. Refined analyses of *syncytin-A*-deficient placentae reveal an alteration of the architecture of the syncytiotrophoblast-containing labyrinth, with overexpansion of trophoblast cells leading to a significant reduction of fetal blood vessel spaces, together with defects in the formation of one of the two interhemal syncytial layers. These findings demonstrate that *syncytin-A* is essential for trophoblast cell fusion and placenta development, and they lend support to a founder role of retroviral gene capture for the evolution of placental mammals.

Results

Embryonic Lethality of *syncytin-A* Knocking Out. We deleted the mouse *syncytin-A* ORF (carried by a single 1.8-kb exon) by homologous recombination using a strategy based on the Cre/LoxP

Author contributions: A.D., C.V., and T.H. designed research; A.D., C.V., O.B., F.H., G.P., and P.O. performed research; A.D., C.V., G.P., P.O., and T.H. analyzed data; and A.D. and T.H. wrote the paper.

The authors declare no conflict of interest.

This article is a PNAS Direct Submission.

See Commentary on page 11827.

[1]A.D. and C.V. contributed equally to this work.

[2]To whom correspondence should be addressed. E-mail: heidmann@igr.fr.

This article contains supporting information online at www.pnas.org/cgi/content/full/0902925106/DCSupplemental.

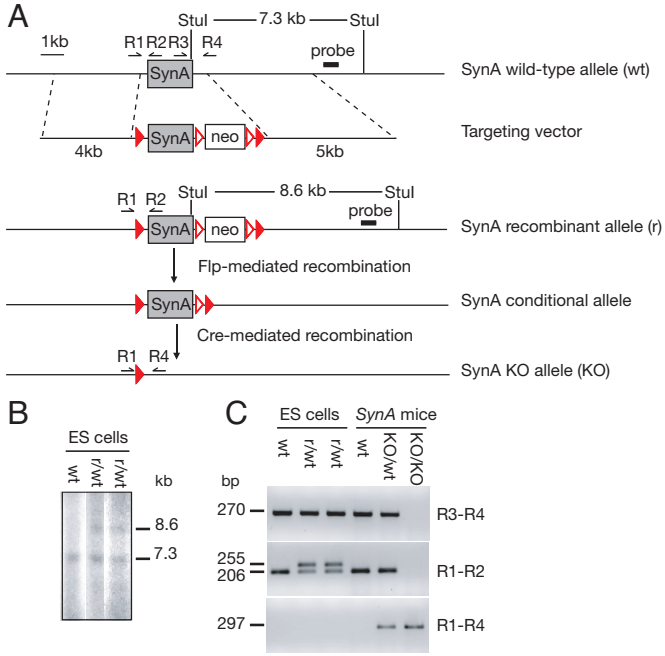

Fig. 1. Targeted disruption of the *syncytin-A* gene. (*A*) Structure of the wild-type (wt) locus, the targeting vector, the targeted recombinant allele (*r*), the conditional allele, and the deleted, knockout (KO) *syncytin-A* (single-exon) allele. The loxP and FRT recombination sites (red and empty triangles, respectively), the StuI restriction sites and probe for Southern blot analysis, and the R1–R4 primers for PCR genotyping are indicated. (*B*) Southern blot analysis of the wild-type (wt) ES cells and of the 2 recombinant (r/wt) clones used to establish independent recombinant mouse lines. StuI-restricted DNA yielded 7.3- and 8.6-kb bands for the wild-type and recombinant alleles, respectively, with the probe in *A*. (*C*) PCR-based genotyping of ES cells and mice (wild-type and knockout) using the R3–R4, R1–R2, and R1–R4 primer pairs indicated in *A* (fragments smaller than 500 bp are shown).

recombination system for generating knockout mice (see Fig. 1 and *Materials and Methods*). Two independent ES cell clones were used to establish germ-line chimera, and both yielded mutant mice with similar phenotypes. Mice bearing the conditional alleles, as well as heterozygous SynA$^{+/-}$ animals, obtained after crossing with Flp-recombinase-expressing and Cre-recombinase-expressing mice (Fig. 1), were viable, fertile, and exhibited no obvious phenotypic defects. Therefore, heterozygosity of *syncytin-A* was phenotypically inapparent. However, in intercrosses of SynA$^{+/-}$ animals, no viable homozygous null offspring were identified, whereas wild-type and heterozygous offspring were obtained at the expected Mendelian ratio, suggesting that loss of both *syncytin-A* alleles is embryonically lethal (Table 1). Examination of the embryos at various stages of gestation revealed that 20% of SynA$^{-/-}$ embryos died by embryonic day 11.5 (E11.5), with this proportion further increasing to 29% and 48% at E12.5 and E13.5, respectively. By E14.5, all SynA$^{-/-}$ embryos were dead (Table 1). These findings show that *syncytin-A* is essential for normal embryonic development.

Morphological and Physiological Defects of SynA$^{-/-}$ Embryos and Extraembryonic Tissues. Noteworthily, the living SynA$^{-/-}$ embryos between E11.5 and E13.5 showed growth retardation, with a body weight reduction of up to 25%, compared with wild-type and SynA$^{+/-}$ embryos that developed normally throughout gestation (Fig. 2 *A* and *B*). Moreover, they were paler (Fig. 2*B*) and displayed decreased vascularization of their extraembryonic annexes. Blood vessels branching at the surface of the yolk sac (Fig. 2 *C* and *D*) and on the fetal side of the placenta (Fig. 2*E*) of mutant embryos were barely visible. These defects were reproducibly observed from

Table 1. Genotypes of offspring from SynA$^{+/-}$ × SynA$^{+/-}$ mating

Day of analysis	Embryos with indicated genotype, total (dead)			Percentage death in −/−
	+/+	+/−	−/−	
E9.5	11	10	7	0
E10.5	11 (1)	22 (1)	8 (1)	12
E11.5	35 (1)	75 (1)	40 (8)	20
E12.5	28	43 (1)	17 (5)	29
E13.5	37 (1)	70 (3)	29 (14)	48
E14.5	25	31 (2)	13 (13)	100
E15.5	7	14	9 (9)	100
E16.5	18	14	14 (14)	100
E18.5	14	11	0*	100
Postnatal†	46	105	0	100

*no −/− embryos detected because of body resorption preventing genotyping.
†Postnatal day 21.

E11.5 to E13.5 (E13.5 embryos in Fig. 2) and could contribute to growth retardation. Consistent with our previous observation that *syncytin-A* is not expressed in the developing embryo but only in the placenta (12), histological examination revealed no gross abnormalities of the mutant embryos, suggesting that an impaired placental function could be the cause of embryonic lethality. Indeed, measurement of transplacental passage by using the fluorescent dye rhodamine 123 injected into the mother (13, 14) revealed a significant ($P < 0.0001$) 15% reduction in the fluorescence recovered in the living E11.5 SynA$^{-/-}$ embryos compared with their wild-type littermates, consistent with reduced placental transport capacity (Fig. 2*F*).

Altered Labyrinth Architecture in SynA$^{-/-}$ Placenta. To further analyze the placental defects, we performed histological analyses of wild-type and SynA$^{-/-}$ placentae between E11.5 and E13.5. The placenta is composed of the maternal decidua and a fetal part that consists of 3 distinct trophoblast compartments: the labyrinth, the spongiotrophoblast, and the giant cell zone (Fig. 3*A*) (2, 4). The labyrinth is the site of oxygen, nutrient, and waste exchanges between maternal and fetal blood. It has a porous aspect, with juxtaposed maternal blood lacunae and fetal blood vessels, separated from each other by well-organized syncytial and mononuclear trophoblastic cell layers (Fig. 3*A*). Fetal blood vessels are easily distinguished from maternal lacunae because they are lined by endothelial cells and contain primitive nucleated erythrocytes. SynA null placentae were of normal size, and the spongiotrophoblast and giant cell zone appeared normal. However, the labyrinth was clearly altered and appeared more compact, with clusters of densely packed trophoblast cells (Fig. 3 *B* and *C*). Accordingly, a significant ($P < 0.0001$) 1.3-fold increase in the number of labyrinthine trophoblast cells was assessed by counting cell nuclei per surface unit (204 ± 6.4, $n = 31$ for mutant vs. 140 ± 4.3, $n = 37$ for wild type; see *Materials and Methods*). In the mutants, the fetal blood vessel spaces were significantly reduced, and the embryonic erythrocytes, less frequently detected, appeared to be squeezed into the narrowed vessels (Fig. 3*C*). These defects are expected to alter the fetal blood flow, accounting for the decreased placental and yolk sac vascularization observed in null embryos and ultimately resulting in their retarded growth and death.

Light microscopy data were corroborated by marker analyses on placenta sections. In situ hybridization demonstrated correct spatial expression of the 4311 (Fig. 3*D*) (15) and mPLI (Fig. 3*E*) (16) marker genes in the spongiotrophoblast and in giant cells, respectively, indicating that these 2 tissues are not affected in mutant placentae. To examine further the vascularization abnormalities in

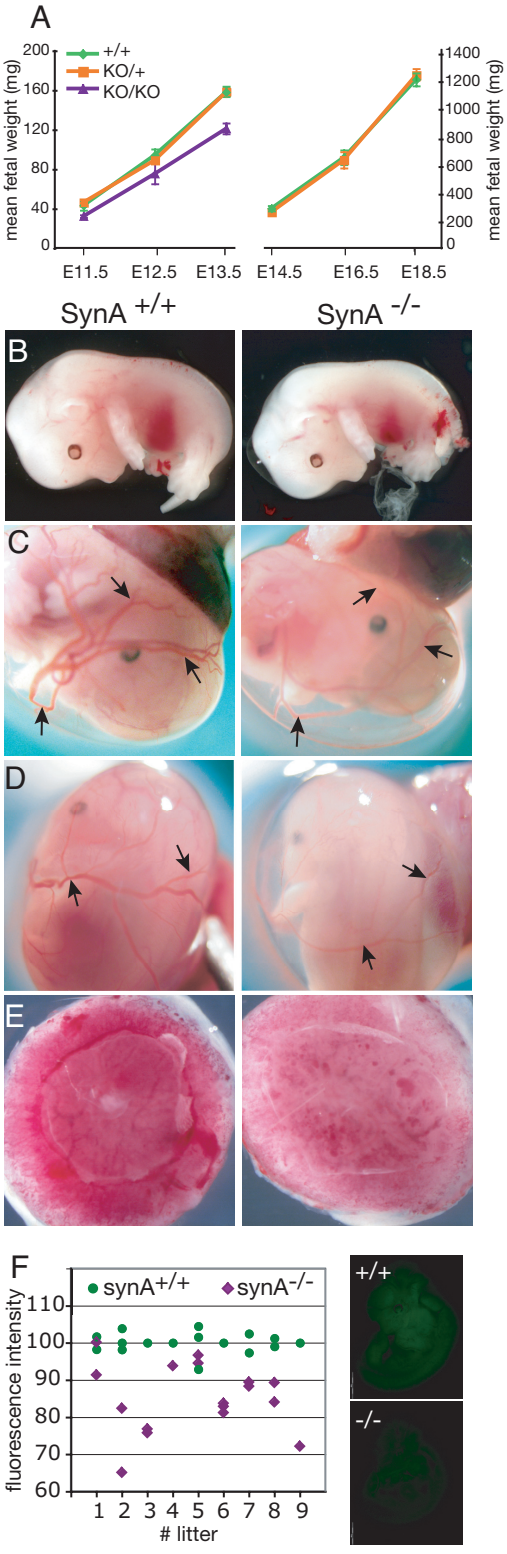

Fig. 2. Morphological and physiological abnormalities of SynA null embryos and extraembryonic tissues. (*A*) Mean fetal weight of wild-type, heterozygous, and SynA null embryos at different embryonic ages (E). Values (milligrams) are means ± SEM of a minimum of 7 living embryos (heart beating): 158 ± 5 for wild-type vs. 121 ± 5 for SynA null embryos ($P = 0.0005$) at E13.5; no difference between wild-type and heterozygous embryos. (*B–E*) Vascularization of E13.5 wild-type (*Left*) and living SynA null (*Right*) embryos and of their extraembryonic annexes. (*B*) A representative SynA null embryo, smaller and slightly paler than its wild-type littermate. (*C* and *D*) Two opposite views of yolk sacs with the blood vessels (arrows) pale and barely visible for the mutant. (*E*) Fetal side of placentae showing reduced vascularization in the mutant. (Original magnification: *B*, 12×; *C* and *D*, 15×; and *E*, 25×.) (*F*) Transplacental passage of rhodamine 123 into E11.5 embryos 2 h after i.p. injection of the fluorescent dye into the mother. (*Right*) Images of representative wild-type and living SynA null embryos from the same litter. (*Left*) Quantification of the fluorescence intensity for wild-type and mutant embryos from 9 independent litters. For each litter, the mean fluorescence intensity of the wild-type embryos is set as 100%, and the relative intensity of each littermate is plotted. Two-tailed unpaired *t* test indicates significant difference ($P < 0.0001$) between wild-type and mutant embryos (mean fluorescence intensity ± SEM: 85.15 ± 2.2, $n = 17$ for mutant vs. 100 ± 0.6, $n = 16$ for wild-type embryos); only living embryos were analyzed.

the labyrinth area, endothelial cells lining the lumen of fetal blood vessels were stained for CD34 (a cell surface marker strongly expressed in vascular endothelial cells and their progenitors) by immunochemistry (Fig. 3 *F* and *G*). Whereas CD34-positive cells appeared regularly scattered in the labyrinth of wild-type placenta, in mutant placenta, extended nonvascularized areas formed by densely packed trophoblast cells were observed (Fig. 3*F*), along with a severe reduction in fetal blood spaces (Fig. 3*G*). Interestingly, the ratio of CD34-expressing cells to total labyrinth areas was not significantly different between wild-type and mutant placentae (4.7% ± 0.6% for wild-type vs. 4.3% ± 1.3% for mutant, $P = 0.8$, at E12.5; 3.9% ± 0.8% for wild-type vs. 5.0% ± 0.3% for mutant, $P = 0.3$, at E13.5), indicating that angiogenesis is not impaired during the course of labyrinth formation in SynA null placentae and that fetal blood vessels are most likely secondarily compressed by the abnormal expansion of trophoblast cells. Actually, Ki67 immunochemistry, used as a marker of proliferating cells, revealed aggregates of positive trophoblast cells in mutant placentae that were not observed in the wild type (Fig. 3*H*). Finally, RT-PCR analysis of a series of labyrinthine trophoblast-specific genes (Fig. S1), revealed no significant differences between wild-type and mutant placentae, except at E12.5 for the GLUT3 glucose transporter (1.8-fold increase; $P = 0.01$) (17) and *mEomesodermin* (1.8-fold increase; $P = 0.005$) (18, 19), a marker of trophoblast stem cells. A lack of differentiation and/or abnormal expansion of these cells could contribute to the phenotype observed in the mutant placenta.

Impaired Syncytiotrophoblast Formation in SynA$^{-/-}$ Placenta. To further characterize the placental defects in the labyrinth, we then examined the fine structure of the interface between fetal blood vessels and maternal lacunae (see scheme in Fig. 3*A Right*) by using electron microscopy. As illustrated in Fig. 4*A*, the labyrinth from E11.5 wild-type placenta showed the typical trilaminar interhemal barrier separating maternal and fetal blood compartments, which consists of a layer of mononuclear sinusoidal trophoblast giant cells (STGCs) and 2 layers of syncytiotrophoblasts (STs), ST-I and ST-II, the latter apposed to the fetal vessel endothelial cells (Figs. 3*A* and 4*A*). The 2 ST layers arise from the fusion of trophoblast cells during labyrinth formation. They differ by their cellular composition, with ST-II containing abundant lipid inclusions, and tightly adhere to each other through frequent desmosomes and gap junctions for intercellular transport (Fig. 4 *A* and *B*). The interhemal barrier of the SynA null placenta shows normal STGCs and fetal endothelial cells surrounding 2 internal layers, one with ST-II features (lipid inclusions, interaction with the fetal endothelium) but the other ill-defined (from now on designated T-I for trophoblast-I layer; Fig. 4 *C* and *D*) and remarkably different from the wild-type ST-I layer (Fig. 4*B*). Notably, T-I discloses an accumulation of irregular membrane structures, and its interface with ST-II is deeply disrupted, with extensive convolutions of the T-I membranes and only few scattered desmosomes and gap junctions (Fig. 4*D*). In rare areas where the T-I layer is less perturbed so that the cell boundaries can be delineated, it can be observed that T-I is

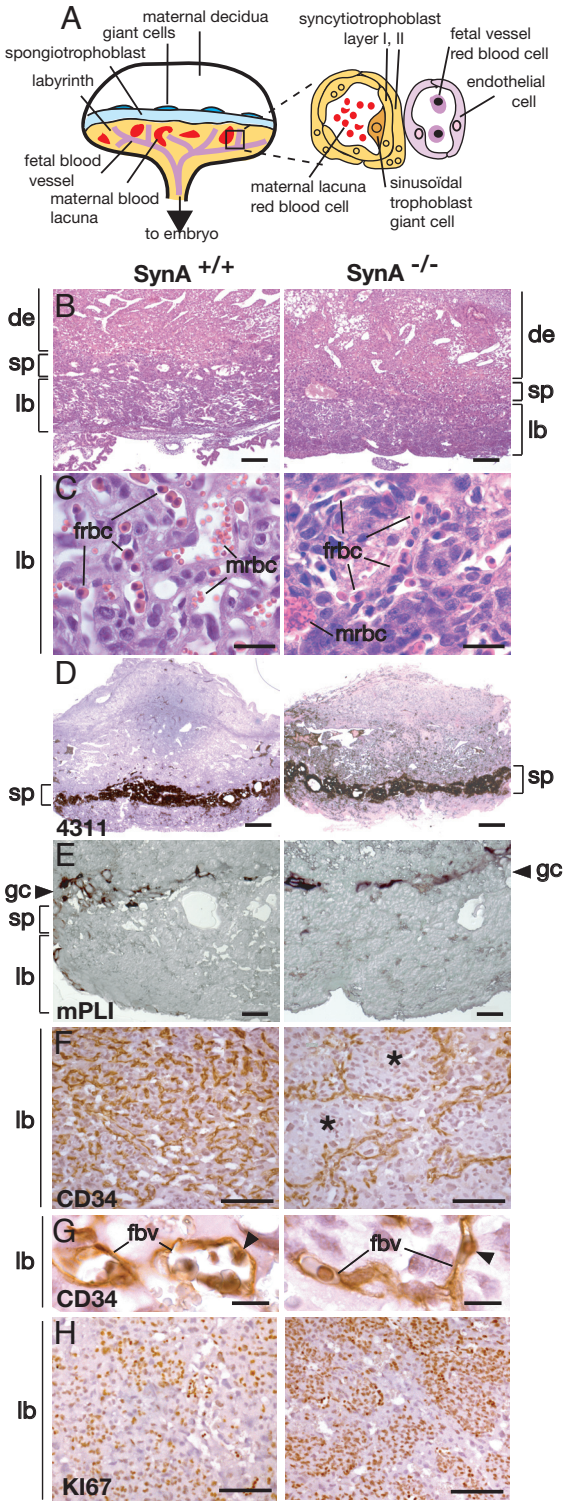

Fig. 3. Placental abnormalities in the labyrinth of SynA null embryos. (*A*) Schematic representation of the mouse placenta (*Left*) including the labyrinth (lb), the spongiotrophoblast (sp), and the giant cells (gc), adjacent to the maternal decidua (de). In the labyrinth (enlarged view on the *Right*), maternal blood lacunae—containing maternal red blood cells (mrbc)—are separated from fetal blood vessels (fbv)—containing fetal red blood cells (frbc)—by a trilaminar barrier composed of mononuclear sinusoidal trophoblast giant cell (stgc) and 2 layers of syncytiotrophoblasts (ST-I and ST-II), the latter apposed to the fetal endothelium. (*B–H*) Light microscopy analysis of wild-type (*Left*) and mutant (*Right*) placental tissues. (*B* and *C*) Hematoxylin/eosin staining of 5-μm placental sections from living E12.5 embryos with the labyrinth, spongiotrophoblast, and maternal decidua delineated. Enlarged view of the labyrinth (*C*), with fetal and maternal red blood cells indicated. The labyrinth of SynA null placenta is more compact, with the fetal red blood cells squeezed inside the narrowed vessels. (*D–H*) Marker analyses by in situ hybridization for 4311 and mPLI (*D* and *E*) or by histochemistry for CD34 (*F* and *G*) and Ki67 (*H*) of placenta sections of E11.5 (*D*, *E*, and *H*) and E13.5 (*F* and *G*) embryos. CD34-negative nonvascularized areas (in *F*) are indicated with asterisks; CD34-positive fetal blood vessels (fbv, see enlarged view in *G*) have a reduced internal space in SynA null labyrinth, with fetal erythrocytes (arrowheads) squeezed. (*H*) Ki67-positive cells forming aggregates in the SynA null labyrinth. (Scale bars: *B* and *D*, 400 μm; *E*, *F*, and *H*, 100 μm; *C*, 25 μm; and *G*, 12.5 μm.)

discontinuous, with unfused membranes apposed (Fig. 4 *E* and *F*, arrows). This is never observed in the wild-type ST-I layer, and it indicates impaired syncytialization in the SynA null placenta. In addition, apoptotic cells with dense, cup-shaped chromatin (Fig. 4*G*) were observed in SynA null but not in wild-type placental labyrinth, consistent with the results of TUNEL assays that we performed on the placentae of wild-type and living mutant E13.5 embryos (>10-fold increase in TUNEL-positive cells in mutant embryos; see Fig. S2). Their position, between the STGC and ST-II layers, suggests that these apoptotic cells originate from nonsyncytial T-I cells. Finally, in some areas, the ST-II layer is observed extending between fetal endothelial cells and undifferentiated mononuclear trophoblast cells (Fig. S3), as expected at this developmental stage (20), further indicating that the ST-II layer develops normally in the mutant labyrinth. In agreement with impaired formation of the ST-I but preservation of the ST-II layer in SynA null mice, *syncytin-A* transcripts were previously detected by in situ hybridization in the labyrinth close to the maternal lacunae, consistent with the ST-I layer, whereas *syncytin-B* and *GCMa* gene expression, which we found unchanged in SynA null mice (Fig. S1), was detected close to the fetal vessels, consistent with the ST-II layer (21).

Discussion

Here, to elucidate the role of syncytin genes in mammalian physiology, we generated mice deficient for *syncytin-A* by gene targeting. Remarkably, null homozygous embryos invariably die at midgestation, between embryonic days 11.5 and 13.5, indicating that *syncytin-A* is required for embryonic development. The cause of embryonic death was found to be defective development of the placenta, consistent with the placental transport defects observed in SynA null embryos and with our previous observations that *syncytin-A* is expressed exclusively in this tissue, being silent in both the developing embryo and adult nonplacental tissues (12). Placenta alterations were detected at the level of the labyrinthine zona, which is the site of fetomaternal exchanges in mature placenta. This is compatible with the fact that SynA null embryos die at midgestation, inasmuch as the labyrinth layer is formed and begins to function as the transport unit at approximately day 11.5 of gestation. During labyrinth formation in the mouse, trophoblast cells fuse to form 2 syncytiotrophoblast layers (ST-I and ST-II) that separate fetal blood vessels and maternal blood lacunae and mediate the fetomaternal exchanges. In the labyrinth of SynA null placenta, we show (*i*) defects in syncytial formation of the ST-I interhemal layer, which can no longer interact properly with ST-II for adequate fetomaternal transport and most probably finally undergoes apoptosis, and (*ii*) an overexpansion of trophoblast cells in the labyrinth at the expense of fetal blood vessel spaces. Both defects could be linked, with the progenitor cells that normally differentiate into the ST-I layer being blocked in their differentiation pathway toward syncytiotrophoblast. They likely contribute to the observed decreased vascularization and placental transport defects, leading ultimately to fetal growth retardation and death of the developing embryo at midgestation.

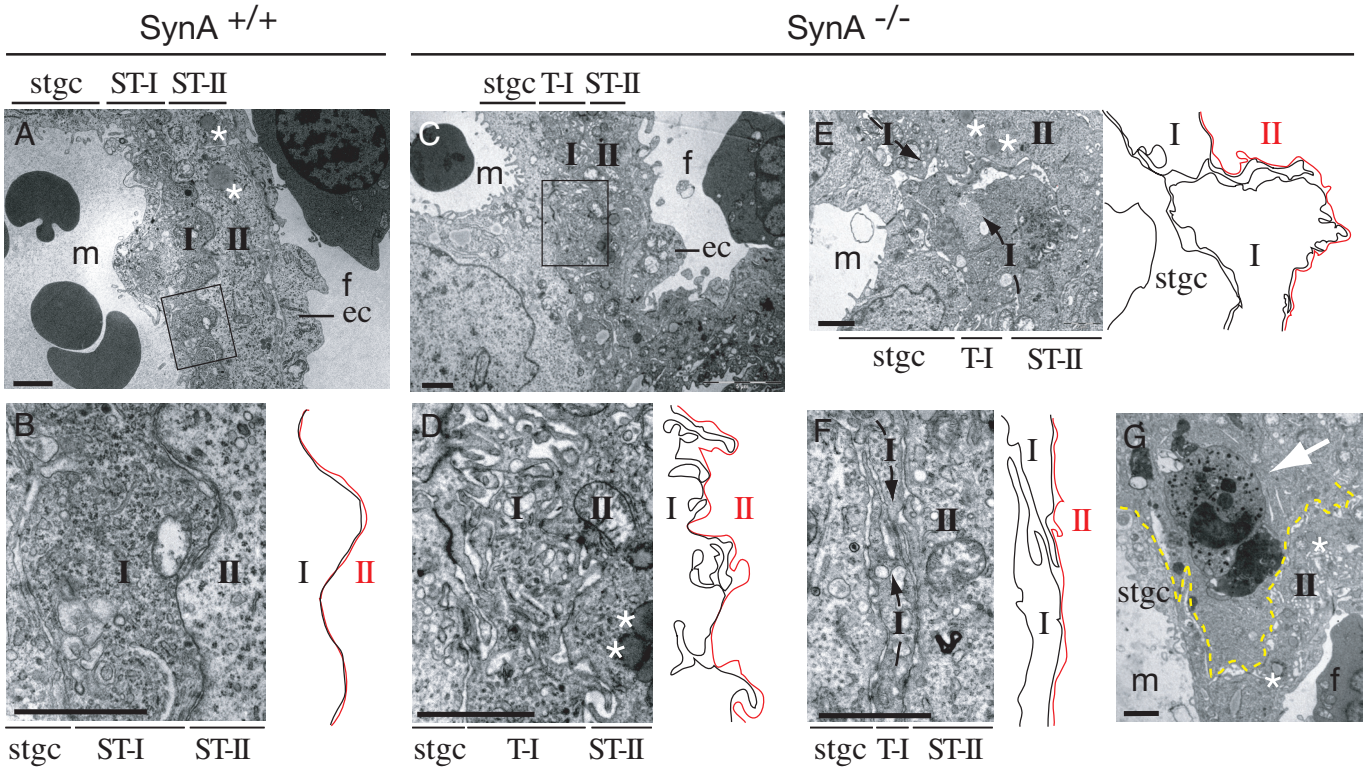

Fig. 4. Electron micrographs of labyrinth of E11.5 wild-type (*A* and *B*) and SynA null (*C–G*) placentae. (*A*) Three-layered interhemal barrier of wild-type labyrinth at the maternofetal interface [m indicates maternal blood lacuna with darkly stained erythrocytes, and f indicates fetal blood vessel lined by endothelial cells (ec) with a nucleated erythrocyte] with the mononuclear sinusoidal trophoblast giant cells (stgc) and the 2 syncytiotrophoblast (ST-I and ST-II) layers delineated, and the ST-II-specific lipid inclusions indicated with asterisks. (*B*) Expanded view of the area boxed in *A*, showing tight apposition of the ST-I and ST-II layers (outlines of the facing cytoplasmic membranes schematized on the *Right*). (*C* and *D*) same as *A* and *B* for the SynA null placenta, with the 3-layered structure still present (*C*) but with severe disturbance of the putative ST-I (T-I) layer and disrupted interactions with ST-II (*D*, facing cytoplasmic membranes outlined on the *Right*); ST-II appears normal (typical lipid inclusions indicated by asterisks). (*E* and *F*) Images of unfused T-I cells as observed in less-disturbed SynA null interhemal domains. Apposed cytoplasmic extensions (arrows) are schematized on the *Right*. (*G*) Apoptotic cell (arrow) with cup-shaped condensed chromatin, in contact (yellow dotted line) with a sinusoidal trophoblast giant cell (stgc) and the ST-II layer. (Scale bars: 2 μm.)

The present knockout mice highlight *syncytin-A* as an essential mediator of placenta development and syncytiotrophoblast formation and provide direct evidence that a gene of retroviral origin is required for a "founding" physiological process. Other captured genes have been reported to be involved in placenta formation; namely, 2 genes from intracellular mobile elements and one gene from an ovine retrovirus, but none of them are involved in syncytiotrophoblast formation. The *Peg10* and *Rtl1* genes derived from the Sushi-ichi-related retrotransposon are conserved in all eutherian mammals, and knockout mice provided evidence for a role of these genes at early and late stages of placental development, respectively (22, 23). In the sheep, the envelope gene of a family of endogenous retroviruses related to the Jaagsieke sheep retrovirus was demonstrated to be involved in periimplantation placental morphogenesis, via loss-of-function experiments using in utero injection of antisense oligonucleotides (24). Although the precise function of these genes remains unknown, these findings strengthen the importance of gene capture from retroelements for placental evolution and reproductive biology.

Here, we identify the *syncytin-A* envelope gene, with its inherited fusogenic activity, as the direct effector of the fusion process involved in the establishment of the syncytial structure, possibly aided by nonstructural cellular genes, such as the previously identified phospholipase C-δ1 and C-δ3 (25) and Gcm1 (26, 27) transcription factor. Interestingly, despite the great morphological diversity of mammalian placentae, a multinucleated syncytiotrophoblast layer is found in several mammalian orders, including even-toed ungulates, carnivores, rodents, lagomorphs, and primates (5, 6). The presence of fusogenic syncytin genes already demonstrated for rodents and primates (9–12) and the present results now provide strong arguments that the cooptation of genes of retroviral origin must have occurred independently and on several occasions during mammalian evolution for the convergent emergence of a common syncytial interhemal barrier.

A still-unanswered question concerns the role of the second murine syncytin gene, *syncytin-B*, which possesses, in addition to a fusiogenic activity, an immunosuppressive activity, as also observed for one of the two human syncytin genes and the envelope gene of infectious retroviruses (28–30). Generation of knockout mice for this gene should provide definitive insights into the respective role of these pairwise conserved genes in placental physiology and, possibly, in maternofetal tolerance, necessarily associated with placentation in mammals. Finally, it should be stressed that in humans, several pathologies, including intrauterine growth retardation, preeclampsia, and Down's syndrome, are associated with altered syncytial formation (3, 31, 32). The present report now provides an animal model for appraising the role of the homologous, retrovirally acquired syncytin genes found in humans in these pathological processes and in normal pregnancy.

Materials and Methods

Gene Targeting. The 4-kb 5′ arm and the 5-kb 3′ arm of the targeting vector, corresponding to sequences bracketing the *syncytin-A* ORF, and a 1.8-kb

syncytin-A ORF-containing fragment preceded by an upstream LoxP site were generated by PCR using primers listed in Table S1 and DNA from a 129/Sv mouse Bac clone (303e12; ResGen, Invitrogen). The targeting vector (Fig. 1) contains the *syncytin-A* and the neomycin resistance (*neo*) genes flanked by FRT and LoxP recombination sites allowing their conditional excision. SynA recombinant mouse lines were established at the Mouse Clinical Institute (Illkirch, France) by using 129S2/SvPas mouse embryonic stem cells. After G418 selection, targeted ES clones were identified by PCR and further confirmed by Southern blot with a 3′ external probe (Fig. 1). Two independent positive ES cell clones were injected into C57BL/6J blastocysts. Male chimaeras positive for germ-line transmission were used to establish 2 independent recombinant mouse lines. The *neo* gene was excised through breeding with Flp recombinase-expressing mice (33), and the *syncytin-A* unique ORF was then deleted through breeding with Cre recombinase-expressing mice (34) (a gift from M. Cohen-Tannoudji, Institut Pasteur, Paris, France). SynA conditional and mutant mice were maintained by crossing with 129/Sv mice. No phenotypic differences were observed between mice derived from the 2 independent ES cell clones.

Histological Analyses. Freshly collected placentae were fixed in 4% paraformaldehyde at 4 °C and embedded in paraffin, and serial sections (4-μm) were stained with hematoxylin and eosin. For cell nuclei counting, 2 wild-type and mutant placentae were examined at 400× magnification: at least 20 fields were scanned at random across the labyrinth (excluding nucleated fetal erythrocytes), and a 2-tailed unpaired *t* test was used for comparison between wild type and mutant. In situ hybridization using digoxigenin-labeled riboprobes was performed on 4-μm paraffin sections according to Roche protocol, with a few modifications (35). For CD34 immunohistochemistry, paraffin sections were processed for heat-induced antigen retrieval, incubated with rat anti-mouse CD34 antibody (Hycult Biotechnology) and rabbit anti-rat antibody (Southern Biotech). Staining was visualized by using the peroxidase/diaminobenzidine Rabbit PowerVision kit (ImmunoVision Technologies). For Ki67 immunochemistry, the processed paraffin sections were incubated with a rabbit monoclonal anti-Ki67 antibody (Neomarkers; LabVision) and stained as above.

Electron Microscopy. Placentae were fixed with 4% glutaraldehyde in 0.1 M cacodylate buffer for 36 h at 4 °C. Specimens were postfixed with 2% osmium tetroxide for 2 h, dehydrated through a graded series of 30% to 100% ethanol, 100% propylene oxide, and then incubated in a 1:1 mixture of propylene oxide–epoxy resin (TAAB). Ultrathin sections (1 μm) were stained with uranyl acetate and lead citrate. Experiments were performed at the Electronic Microscopy Platform, Institut Jacques Monod (Paris, France). Sections were examined with a FEI-Phillips Tecnai 12 or a Zeiss 902 microscope.

Transplacental Passage of Rhodamine 123. Pregnant mice from heterozygous matings were injected i.p. at E11.5 with rhodamine 123 (1 μg/g of body weight; Sigma–Aldrich). At high concentration, this dye shows passive mother-to-fetus passage (13, 14). Mice were killed 2 h after injection, and living embryos (heart beating) were analyzed with a fluorescence stereomicroscope (SZX12; Olympus). The fluorescence intensity in the embryo (ratio of total embryonic fluorescence to embryonic surface) was measured with the Cell-D software (Olympus). Embryos were then processed for genotyping. For each litter, the mean fluorescence intensity of the wild-type embryos was set as 100%, and the relative intensity of each wild-type and mutant littermate was calculated. A 2-tailed unpaired *t* test was used for comparison between mutant and wild type.

ACKNOWLEDGMENTS. We thank M. Cohen-Tannoudji for the gift of plasmids, the Cre recombinase transgenic mice, and helpful discussions; F. Petit (Hospital Béclère, Clamart, France) for the in situ hybridization technique; J. Rossant (Hospital for Sick Children, Toronto, Canada) for providing in situ hybridization probes; I. Godin (Institut Gustave Roussy) for technical support; and the Service Commun d'Expérimentation Animale (Institut Gustave Roussy) for animal care. We are grateful to D. Hernandez-Verdun and C. Kanellopoulos for valuable discussions, and M. San Roman for skillful technical assistance. We thank C. Lavialle for comments and critical reading of the manuscript. This work was supported by the Centre National de la Recherche Scientifique and the Ligue Nationale Contre le Cancer (Equipe ''labellisée'').

1. Huppertz B, Tews DS, Kaufmann P (2001) Apoptosis and syncytial fusion in human placental trophoblast and skeletal muscle. *Int Rev Cytol* 205:215–253.
2. Georgiades P, Ferguson-Smith A, Burton G (2002) Comparative developmental anatomy of the murine and human definitive placentae. *Placenta* 23:3–19.
3. Bischof P, Irminger-Finger I (2005) The human cytotrophoblastic cell, a mononuclear chameleon. *Int J Biochem Cell Biol* 37:1–16.
4. Watson ED, Cross JC (2005) Development of structures and transport functions in the mouse placenta. *Physiology* (*Bethesda*) 20:180–193.
5. Leiser R, Kaufmann P (1994) Placental structure: In a comparative aspect. *Exp Clin Endocrinol* 102:122–134.
6. Carter AM, Enders AC (2004) Comparative aspects of trophoblast development and placentation. *Reprod Biol Endocrinol* 2:46.
7. Gifford R, Tristem M (2003) The evolution, distribution and diversity of endogenous retroviruses. *Virus Genes* 26:291–315.
8. de Parseval N, Heidmann T (2005) Human endogenous retroviruses: From infectious elements to human genes. *Cytogenet Genome Res* 110:318–332.
9. Mi S, et al. (2000) Syncytin is a captive retroviral envelope protein involved in human placental morphogenesis. *Nature* 17:785–789.
10. Blond JL, et al. (2000) An envelope glycoprotein of the human endogenous retrovirus HERV-W is expressed in the human placenta and fuses cells expressing the type D mammalian retrovirus receptor. *J Virol* 74:3321–3329.
11. Blaise S, de Parseval N, Bénit L, Heidmann T (2003) Genomewide screening for fusogenic human endogenous retrovirus envelopes identifies syncytin 2, a gene conserved on primate evolution. *Proc Natl Acad Sci USA* 100:13013–13018.
12. Dupressoir A, et al. (2005) Syncytin-A and syncytin-B, two fusogenic placenta-specific murine envelope genes of retroviral origin conserved in Muridae. *Proc Natl Acad Sci USA* 102:725–730.
13. Pavek P, et al. (2003) Examination of the functional activity of P-glycoprotein in the rat placental barrier using rhodamine 123. *J Pharmacol Exp Ther* 305:1239–1250.
14. Tanaka H, et al. (2005) Hepatocyte growth factor activator inhibitor type 1 (HAI-1) is required for branching morphogenesis in the chorioallantoic placenta. *Mol Cell Biol* 25:5687–5698.
15. Lescisin KR, Varmuza S, Rossant J (1988) Isolation and characterization of a novel trophoblast-specific cDNA in the mouse. *Genes Dev* 2:1639–1646.
16. Colosi P, et al. (1988) Characterization of proliferin-related protein. *Mol Endocrinol* 2:579–586.
17. Shin BC, et al. (1997) Glucose transporter GLUT3 in the rat placental barrier: A possible machinery for the transplacental transfer of glucose. *Endocrinology* 138:3997–4004.
18. Tanaka S, et al. (1998) Promotion of trophoblast stem cell proliferation by FGF4. *Science* 282:2072–2075.
19. Russ AP, et al. (2000) Eomesodermin is required for mouse trophoblast development and mesoderm formation. *Nature* 404:95–99.
20. Hernandez-Verdun D (1974) Morphogenesis of the syncytium in the mouse placenta. Ultrastructural study. *Cell Tissue Res* 148:381–396.
21. Simmons DG, et al. (2008) Early patterning of the chorion leads to the trilaminar trophoblast cell structure in the placental labyrinth. *Development* 135:2083–2091.
22. Ono R, et al. (2006) Deletion of Peg10, an imprinted gene acquired from a retrotransposon, causes early embryonic lethality. *Nat Genet* 38:101–106.
23. Sekita Y, et al. (2008) Role of retrotransposon-derived imprinted gene, Rtl1, in the feto-maternal interface of mouse placenta. *Nat Genet* 40:243–248.
24. Dunlap KA, et al. (2006) Endogenous retroviruses regulate periimplantation placental growth and differentiation. *Proc Natl Acad Sci USA* 103:14390–14395.
25. Nakamura Y, et al. (2005) Phospholipase C-δ1 and -δ3 are essential in the trophoblast for placental development. *Mol Cell Biol* 25:10979–10988.
26. Anson-Cartwright L, et al. (2000) The glial cells missing-1 protein is essential for branching morphogenesis in the chorioallantoic placenta. *Nat Genet* 25:311–314.
27. Schreiber J, et al. (2000) Placental failure in mice lacking the mammalian homolog of glial cells missing, GCMa. *Mol Cell Biol* 20:2466–2474.
28. Mangeney M, Heidmann T (1998) Tumor cells expressing a retroviral envelope escape immune rejection in vivo. *Proc Natl Acad Sci USA* 95:14920–14925.
29. Blaise S, Mangeney M, Heidmann T (2001) The envelope of Mason-Pfizer monkey virus has immunosuppressive properties. *J Gen Virol* 82:1597–1600.
30. Mangeney M, et al. (2007) Placental syncytins: Genetic disjunction between the fusogenic and immunosuppressive activity of retroviral envelope proteins. *Proc Natl Acad Sci USA* 104:20534–20539.
31. Frendo JL, et al. (2000) Defect of villous cytotrophoblast differentiation into syncytiotrophoblast in Down's syndrome. *J Clin Endocrinol Metab* 85:3700–3707.
32. Langbein M, et al. (2008) Impaired cytotrophoblast cell–cell fusion is associated with reduced Syncytin and increased apoptosis in patients with placental dysfunction. *Mol Reprod Dev* 75:175–183.
33. Dymecki SM (1996) Flp recombinase promotes site-specific DNA recombination in embryonic stem cells and transgenic mice. *Proc Natl Acad Sci USA* 93:6191–6196.
34. Lallemand Y, Luria V, Haffner-Krausz R, Lonai P (1998) Maternally expressed PGK-Cre transgene as a tool for early and uniform activation of the Cre site-specific recombinase. *Transgenic Res* 7:105–112.
35. Petit FG, et al. (2007) Deletion of the orphan nuclear receptor COUP-TFII in uterus leads to placental deficiency. *Proc Natl Acad Sci USA* 104:6293–6298.